A Newly Designed Electron-Beam-Guiding Ion Source

A Newly Designed Electron-Beam-Guiding Ion Source

Tohru KISHI*

(Received November 15, 1987)

A newly designed ion gun using a trapping function of a potential valley produced by an electron beam used for bombarding a sample material, evaporating the bombarded part and ionizing the evaporated atoms, was examined using computer simulations and experiments. By giving an appropriate bias potential to each electrode constructing an ion source, the electron and back stream ion beams could be simultaneously focused. The experiments showed that the results obtained by the computer simulation could be realized and the order of $10^{-7} \sim 10^{-8}$ A for an ion beam current could be obtained through the center of a tantalum pipe cathode of 0.6 mm inner diameter.

1. Introduction

During the past decade, ion beam technology has made great progress in versatile fields, for example, diagnostics of material components, so-called proton back scattering method, energy spectroscopy of scattered ions, ion beam micro-analyser and the ion beam implantation to fablicate *LSI* tips. With the development of ion technology, many papers have been presented[1-7]. Excited with these movements, the author has also been involved in such problem and already published several papers on an electron-beam-guiding ion source[8-15]. However, since many problems still exist, the author has designed a new ion source and examined the best operating conditions using computer simulations and checked experiments. In the ion gun proposed here, the incident electron beam and back stream ion beam are required to be simultaneously focused by the same focusing system. The possibility of such a condition was firstly persued by computer simulations. Secondly, experiments were carried out based upon the data obtained by the computer simulations. The results will be written in the following sections.

2. Geometry and Principle of the Ion Source

The ion source construction is shown in Fig. 1. Though the principle of the ion source was already published, it will be briefly introduced to help general comprehension. Electrons emitted from one end surface of a pipe cathode K or spiraly wound coil cathode are focused onto a target material T through an electrostatic focusing lens consisting of electrodes A_1 and A_2. If the power of the incident electron beam is great enough and the beam is concentrated into a small area, the bombarded part is heated and evaporated to be ionized by collisions with the incident and/or the secondary electrons emitted from the target. The energy of the ion acquired from the collision with the incident electrons is given by[16]

* Department of Electrical Engineering, College of Engineering.

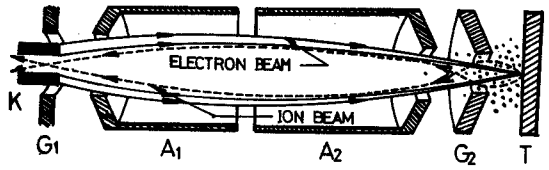

Fig. 1 Schematic construction of an ion gun. K: Cathode, G_1: First control grid for electron beam, A_1 and A_2: Lens electrodes, G_2: Second control grid for ion beam, and T: Target.

$$E_i/E_e = 2\, m_e/M_i \tag{1}$$

where, E_i, E_e, m_e and M_i are the ion energy, the energy of the incident electron, the mass of electron and the mass of ion, respectively. Further, the potential depth V_o produced in the electron beam cloud carrying the electron beam current I_e is given by[17]

$$V_o = (1/4\pi\epsilon_0\, (m_e/2q\, V_e)^{1/2}\, I_e \tag{2}$$

where, ϵ_0, q and V_e are the permittivity of the free space, the charge of the electron, and the acceleration voltage of the electron, respectively. Tables I and II show the relationships between these values. For example, if the acceleration voltage V_e and the electron

Table I

Mass Number	E_i (eV)	
	V_e = 5 kV	V_e = 10 kV
2	2.71	5.43
4	1.35	2.71
18	0.31	0.61
28	0.19	0.38

Table II

Electron Beam Current	Potential Depth V_0	
I_e (mA)	V_e = 5kV	V_e = 10 kV
0.5	0.11	0.08
1.0	0.21	0.15
5.0	1.06	0.75
10.0	2.12	1.51

beam current I_e are 5 kV and 5 mA respectively, the potential depth V_o in the electron beam is 1.06 eV. The ions whose mass number is larger than 6 will be almost perfectly trapped in the electron beam. Of course, the ions less than the mass number 6 are trapped partly because eq. (1) is given statistically, and the initial direction of the ions will be distributed according to the cosine law[18]. On the other hand, the ion current I_i obtained by filling out the potential valley will be given by

$$I_i = (m_e/M_i)\, I_e \tag{3}$$

When the produced number of ions is large enough, excess ions will move according to the law of optics of charged particles. In short, the electrons and ions will move in a given potential distribution considering the effect of the space charge of the electrons and ions. However, as seen from Fig. 1, since the ion beam is taken through the small

center hole of the cathode, the ion beam must be focused into its hole. Therefore, it is a pourpose of this paper to find an electrode system and an operation condition which fullfil simultaneous focusing for the electron and ion beams moving reversely in the same space. As a first step, trajectories of the electron and ion were followed in a given electrode system in which two electrodes A_1 and A_2 were introduced to act as a focusing lens not only for the electrons but also for the ions. The potential applied to each electrode and expectable potential distribution on the optical axis are given in Fig. 2. Further, optical modes for the electron and ion beams are shown in Fig. 3 (a) and (b), respectively. Furthermore, for the cathode, a small tantalum pipe of 1.5 mm and 1.0 mm as an outer and inner diameters, respectively, was assumed.

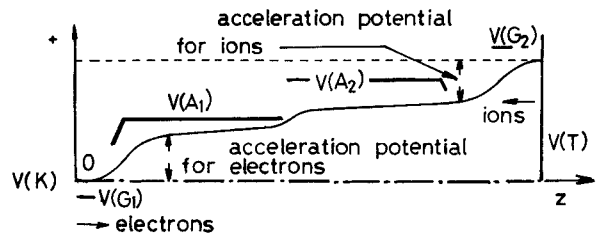

Fig. 2 Potentials given to each electrode and an expected axial potential distribution. The potential of cathode $V(K)$ is assumed zero.

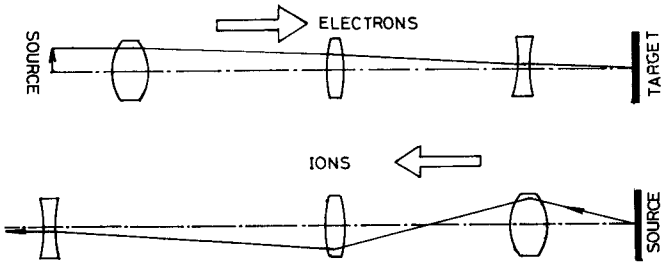

Fig. 3 Optical models for the electron beam (upper) and for the ion beam (lower), respectively.

3. Trajectories of the Incident Electron Beam and Back Stream Ion Beam by Computer Simulations

Since the electrode's geometry of the ion source is circular symmetric, the potential $V(r, z)$ in the referenced space is given by Poisson's equation

$$\frac{d^2V}{dz^2}+\frac{1}{r}\frac{d}{dr}\left(r\frac{dV}{dr}\right)=-\frac{\rho}{\epsilon_0} \tag{4}$$

where, r, z and δ are the radius, optical axis of the system and charge density, respectively. Of course, the charge density contains the sum of the electron and ion charges. If the boundary conditions are given, the above differential equation can be solved numerically with help from the computer. If the potential distribution $V(r, z)$ is obtained, the trajectories of the electron and ion particles are given by equations of

motion.
For the electron,

$$d^2 r_e/dt^2 = -(q/m_e)\,dV/dr_e \tag{5}$$

$$d^2 z_e/dt^2 = -(q/m_e)\,dV/dz_e \tag{6}$$

for the ion,

$$d^2 z_i/dt^2 = (q/M_i)\,dV/dr_i \tag{7}$$

$$d^2 z_i/dt^2 = (q/M_i)\,dV/dz_i \tag{8}$$

where, subscripts e and i correspond to the electron and ion particles, respectively. In this case, the electrons start to move from the cathode surface K with no initial velocity to the target T. On the other hand, the ions start from the target within a spot area produced by the focused electron beam to the cathode K. Therefore, z_i in Eq.(8) should be taken from the T to the K. The first step, Eq.(3), is solved numerically under a condition of $\rho = 0$ using relaxation method[19–23]. Using the distribution $V(r, z)$, Eqs.(4) and (5) are solved and the most outside trajectory is obtained. If 2 mA is assumed as the total electron beam current and the density of it is uniform inside each cross section, a new potential distribution will be obtained by repeating similar calculations. These processes were repeated to reach an error of 2% and 5% for the potential distributions and the trajectories, respectively. The ion beam trajectories were calculated by a similar method, but for initial conditions, an energy of 0.5 eV and directions of 15°, 30° and 45° were assumed, respectively. Further, considering the ion beam current obtained experimentally was in the order of $10^{-7} \sim 10^{-8}$ A, the charge density of the ion beam could be ignored in the real calculations.

A few results obtained by the above calculations are shown in Fig. 4 (a), (b) and (c). In reality, many trajectories were drawn but for simplicity only limitted trajectories were picked up in the figure. Figures 4 (a) and (c) show cases in which the ion trajectories do not focus at the cathode surface, though the electron trajectories focus at the target. Figure 4 (b) corresponds to a case where both the electron beam and ion beam are focused simultaneously. From these trajectories, diameters of the electron beam on the cathode surface and ion beam on the target are shown in Fig. 5 (a) and (b), respectively, as functions of $V(A_1)/V(A_2)$ and $V(G_2)$–$V(T)$. Since the inner radius of the pipe cathode is 0.5 mm, it is clear that the ion beam can pass through the cathode center under appropriate conditions. Influence of the voltage ratio $V(A_1)/V(A_2)$ on the focus of the electron beam is stronger than for the case of the ion beam shown in Fig. 5 (a). Further, Fig. 5 (b) shows that the potential on G_2 has a strong effect on focusing the ion beam.

4. Experimentals

In the previous section, the author has discussed the problem from the viewing point of trajectories of the charged particles, and it was concluded that there were simultaneous focused conditions for the electron and ion beams by giving appropriate bias

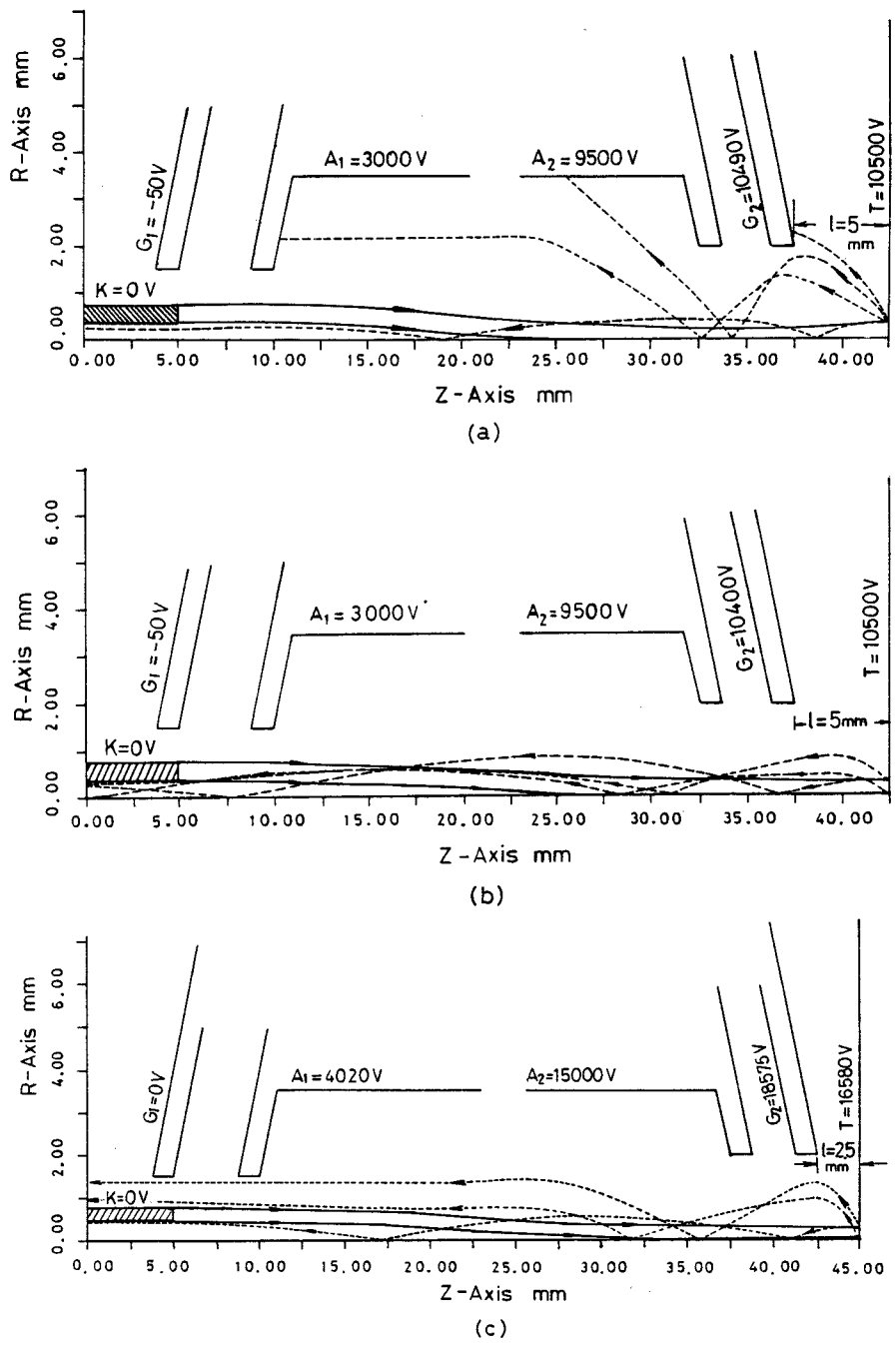

Fig. 4 Electron and ion beam trajectories given by computer simulations.

(a): Focused electron beam and unfocused ion beam. Space 1 is 5 mm.

(b): Focused electron beam and focused ion beam. Space 1 is 5 mm.

(c): Focused electron beam and unfocused ion beam. Space 1 is 2.5 mm.

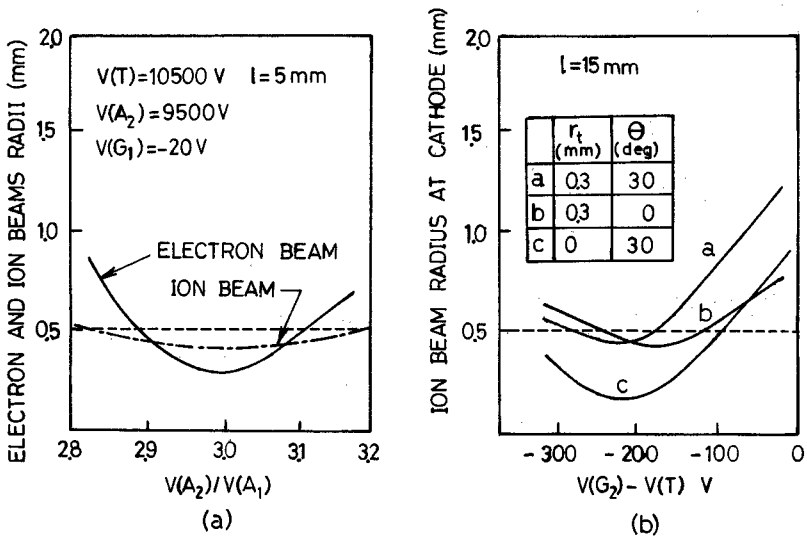

Fig. 5 Electron and ion beams radii at the target and cathode surface, respectively.
(a): Electron and ion beams radii versus the potential ratio $V(A_1)/V(A_2)$.
(b): Ion beam radius at the cathode surface versus the potential difference $V(G_2)-V(T)$.

potential to each electrode. However, several assumptions were introduced in the calculation. First, influences of the grid, G_1, on the total electron beam current and of the secondary electrons from the target on the ionization were ignored. Second, it was assumed that the ion specie contained in the ion beam was only single 28 amu, and third, the velocity distribution of the generated ions and ionization efficiency were not considered. Therefore, the synthetic characteristics of the proposed ion gun should be examined experimentally.

Then, an electrode system similar to Fig. 1 was constructed and a thin Mg plate was used as a target material. A used gun housing is shown in Fig. 6. In the figure, a cross section of a pipe shows a tantalum cathode of 1.0 mm and 0.6 mm as the outer and inner diameters, respectively. Of course, the used gun system was reduced according to the ratio 2/3 which corresponds to the ratio of the real cathode diameter used for the calculation. Therefore, applied potentials were also changed according to the scaling law[24]. Details near the edge of the emitting end of the cathode are shown in Fig. 7. Heater current is symmetrically sent through several tungsten plates to the cathode rod. The thickness of the plate is 0.2 mm and the contact area of each plate is in the order of 10^{-2} mm^2. This small contact area prevents heat flow from the cathode. Possible heater current to be sent through such an edge should be maintained experimentally at less than 10A. If the contact area becomes large, the temperature of the cathode decreases even though fairly high heater current is maintained. Therefore, the life of a cathode is controlled by the increase of the contact area. In other words, if the life of the cathode is defined such that the necessary heater current must be increased to 120% of the initial value because of the increase of the contact area, the cathode could be used no less than 50 ~ 60 hours.

The experiment was performed in a bell-jar. The construction is shown in Fig. 8. Obtained results are shown in Figs. 9 (a), (b) and (c). These figures show only the ion

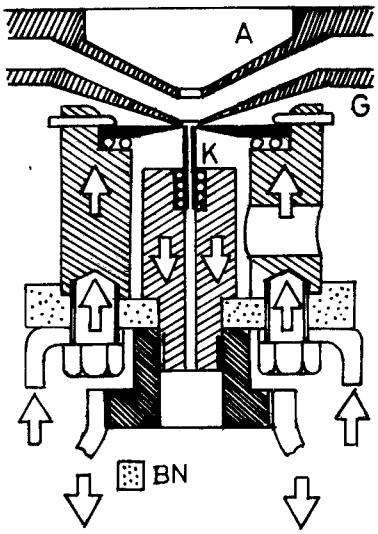

Fig. 6 Electron gun housing (Arrows show paths of heater current).

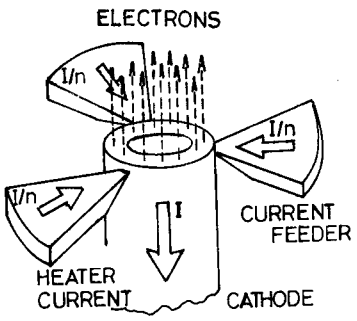

Fig. 7 Details of the end of pipe cathode.

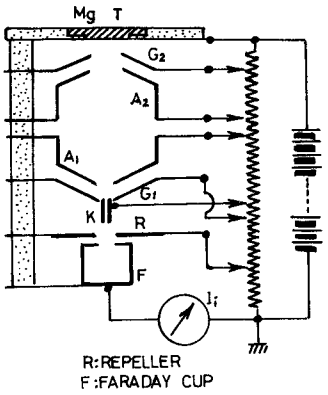

Fig. 8 Experimental set up.

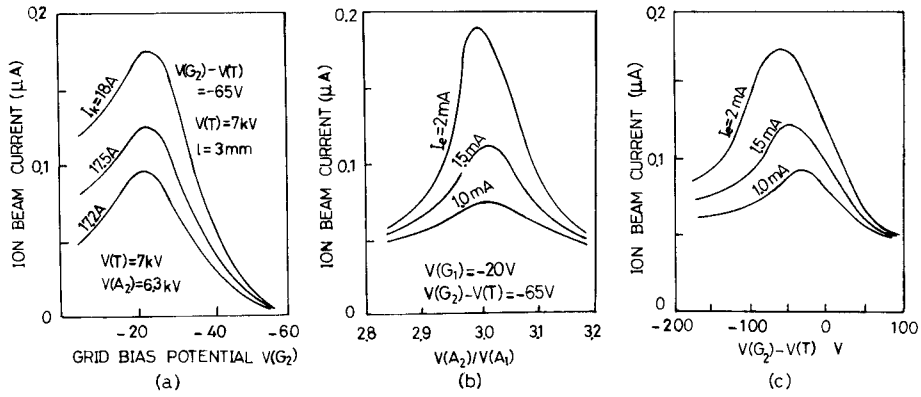

Fig. 9 Experimental results.
(a): Ion beam current versus $V(G_1)$.
(b): Ion beam current versus $V(G_2) - V(T)$.
(c): Ion beam current versus $V(A_1)/V(A_2)$.

current versus $V(G_1)$, $V(G_2)$ and $V(A_1)/V(A_2)$. In each case, the ion beam current shows a peak which corresponds to the focused condition obtained in the calculation. When the ion beam was analysed through an energy filter and a switch magnet, contained ion species are shown in Fig. 10. Magnesium ion peaks (amu = 24, 25 and 26) appear in an electron beam current larger than about 2 mA. Other peaks like H, H_2,

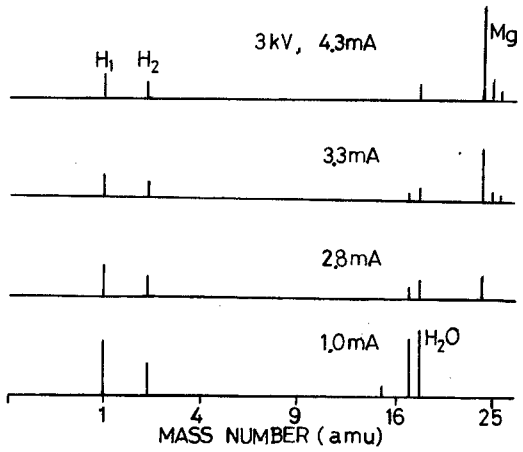

Fig. 10 Mass distribution of obtained ion beam from a Mg target.

N^{14}, HO, H_2O, ... indicate residual gas components contained in the bell-jar.

5. Discussions and Conclusion

As discussed in the previous sections, by inserting a bipotential lens system between the electron gun and the target material around which the ions generated, the possibility of simultaneously focusing the electron and back stream ion beams was examined using computer simulations and experiments. By designing an appropriate electrode geometry and applying an adequate potential to each electrode, it was concluded that the above requirement was fulfilled. The experiment was performed with an electrode system reduced to 2/3 of the model used in the calculation. The diameter of the focused electron beam was about 0.5 mm which was of the order of the value predicted from the calculation. The order of the obtained ion beam current taken through the small inner diameter of 0.6 mm of a Ta pipe cathode was of the order of 0.5×10^{-6} A where a Mg plate was bombarded by an electron beam of 3 kV and 3.5 mA. From spectroscopic analysis, it became clear that about 70% of the obtained ion beam was Mg ions and the remained 30% was residual gas ions in the bell-jar and the impurities contained in the sample material.

This type of ion source will be available for mass spectrometry of small material samples or for obtaining ions from a high melting point material. Further, it will be possible to reduce an obtainable electron beam spot size and to increase an obtainable ion beam current by applying a higher acceleration voltage, for example, 30 kV or 40 kV.

Acknowledgement

The author would like to express thanks to Mr. H. Kamato for his helping on programmings and calculations. This work was partially supported by a Grant-in-Aid for a research on a high brightness ion source using trapping functions of an electron beam (1984 – 1985) from the Ministry of Education.

References

1) J. Worster, Int. J. Electronics, **28**, 117 (1970).
2) K.O. Nielson, Nucl. Instr. Methods, **1**, 289 (1957).
3) S. Ogawa, Nucl. Instr. Methods, **16**, 227 (1962).
4) F.M. Penning, Physica, **4**, 1190 (1937).
5) G. Sidenius, *Proc. Intern. Conf. on Ion Source*, Saclay (1969).
6) E.W. Müller and T.T. Tong, *Field Ion Microscopy* (Elsevier, New York) 1969.
7) L.K. Verheij, Surface Science, **84**, 408 (1979).
8) T. Kishi, T. Nishida and N. Tanizuka, Japan J. Vacuum, **16**, 249 (1975).
9) T. Kishi, I. Yamada and T. Takagi, J. Vac. Sci. Technol., **12**, 954 (1975).
10) T. Kishi, T. Takagi, *Proc. of Intern. Conf. on Ion and Assoc. Technol.*, (Kyoto, Sept., 1984) pp. 389–392.
11) T. Kishi, T. Takagi and I. Yamada, Rev. Sci. Instrum., **50**, 1517 (1979).
12) T. Kishi and T. Takagi, J. Appl. Phys., **53**, 7136 (1982).
13) T. Kishi and T. Takagi, J. Vac. Sci. Technol., **21**, 91 (1982).
14) T. Kishi, *1st China-Japan Joint Conf. on Mass Spectrum.*, (Beijing, Aug., 1984) pp. 145–148.
15) T. Kishi, Ionics, **8**, 16 (1985).
16) D.P. Smith, Surface Science, **25**, 171 (1971).
17) P. Hedval, J. Appl. Phys., **15**, 721 (1944).
18) H. Schwartz, J. Appl. Phys., **35**, 2020 (1964).
19) G. Liebmann, *Field plotting and ray tracing in electron Optics – A review of numeric methods, Advances in Electronics II*, New York, Academic (1950).
20) C. Weber, *Numerical solution of Laplace's and Poisson's equation and calculation of electron trajectories and electron beam, Focusing of charged particles*, New York, Academic Press (1967).
21) A.V. Crewe, D.N. Eggenberger and L.M. Welter, Rev. Sci. Instrum., **39**, 433 (1968).
22) R. Hutter, *Focusing of charged particle ed. by* A. Septier (Academic Press, New York, 1967) Vol. II, pp. 74–76.
23) R. Speidal, G. Kilger and E. Kasper, Optik, **54**, 433 (1980).
24) H. Moss, *Narrow angle electron guns and cathode ray tubes* (Academic Press, New York, 1968) p. 132.